Dual-Band Circularly-Polarized Shared-Aperture Array for C/X-Band Satellite Communications

Chun-Xu Mao, Steven Gao, *Senior Member, IEEE*, Yi Wang, *Senior Member, IEEE*, Qing-Xin Chu, *Senior Member, IEEE*, Xue-Xia Yang, *Member, IEEE*

***Abstract*—A novel method of achieving a single-feed circularly-polarized (CP) microstrip antenna with both broad impedance bandwidth and axial ratio (AR) bandwidth is presented. The CP characteristics are generated by employing a resonator to excite the two orthogonal modes of the patch via two coupling paths and the required 90º phase difference is achieved by using the different orders of the two paths. The presented method, instead of conventional methods that power dividers and phase delay lines are usually required, not only significantly enhances the bandwidths of the antenna, but also results in a compact feed, reduced loss and high gain. Based on this method, a dual-band shared-aperture CP array antenna is implemented for C/X-band satellite communications. The antenna aperture includes a 2 × 2 array at C-band and a 4 × 4 array at X-band. To accommodate the C/X-band elements into the same aperture while achieving a good isolation between them, the C-band circular patches are etched at the four corners. The measured results agree well with the simulations, showing a wide impedance bandwidth of 21% and 21.2% at C- and X-band, respectively. The C- and X-band 3-dB AR bandwidths are 13.2% and 12.8%. The array also exhibits a high aperture efficiency of over 55%, low side-lobe (C-band: -12.5 dB; X-band: -15 dB) and high gain (C-band: 14.5 dBic; X-band: 17.5 dBic).**

***Index Terms*—Dual-band, broadband, circularly-polarized, microstrip antenna, shared-aperture, satellite communication.**

I. Introduction

SATELLITE communication systems play an important role in our daily lives as they deliver many essential services, such as remote telephone connection, live television, radio broadcasting, and Internet access. In order to reduce the cost, the satellites should be able to operate in multiple frequency bands. Broad bandwidth is also desired to increase the capacity of wireless systems. For satellite communication, circularly polarized (CP) antenna is required for its immunity to antenna orientation and the ability to reduce multi-path effects [1]-[2]. In circumstances such as small satellites and user terminals, where space is very limited, multi-band antennas with compact size, light weight and shared aperture are particularly desired [3]-[4].

Over the last decade, various types of dual-band CP antennas have been reported for multi-band operations. Among them, CP slot antennas have the advantages of low profile and simple structure [5]-[7]. But they are usually bi-directional and have a low gain. To overcome these drawbacks, microstrip antennas have been adopted to achieve the unidirectional radiation and high gain [8]-[14]. However, most of these reported CP microstrip antennas suffer from narrow impedance bandwidth and axial ratio (AR) bandwidth. In addition, most of these CP antennas always have a low frequency ratio less than 1.5, which limits their applications in dual-band array antennas.

Several dual-band CP antenna arrays with shared aperture have been reported. In [15], three triangular patches of each band were rotated and sequentially fed. In [16], the two orthogonal modes of the rectangular patches were individually excited and sequentially rotated, forming a dual-band aperture shared array. In [17], the radiation elements for different bands were combined together into a dual-band element, which was then expanded to an array antenna using the sequential rotation technique. Dual-band CP array was also achieved by loading stubs on the CP radiation elements [18]. For all these dual-band CP arrays, the radiator numbers as well as the element spacing are identical for the both bands, which usually leads to a low aperture efficiency and high side-lobe at the high-band. In addition, it is very challenging to achieve the broad impedance and AR bandwidths at both bands, simultaneously.

To obtain a dual-band CP array antenna with the broadband impedance/AR bandwidths, high aperture efficiency and low side-lobe level at both operations, the first and foremost requirement is that the antenna should have the individual radiators and feed networks for the two bands. This, however, will lead to the congestion of the radiation elements and feeding networks in the shared aperture [19]-[20]. Thus, the CP antenna element with a single feed is the only candidate in this work as the traditional dual-fed methods usually occupy a large area for accommodating the power dividing networks and phase-delay lines. In addition, broad impedance bandwidth and 3-dB AR bandwidth are simultaneously required at both frequency bands. All these challenging tasks need to be overcome in this work.

In this paper, a dual-band CP array antenna with shared

Manuscript submitted on April 26, 2017; This work is supported by UK EPSRC grant EP/N032497/1 and YW is supported by UK EPSRC under Contract EP/M013529/1.

C. X. Mao and S. Gao are with School of Engineering and Digital Arts, University of Kent, UK (email: cm688@kent.ac.uk; s.gao@kent.ac.uk).

Y. Wang is with the Department of Engineering Science, University of Greenwich, UK.

Q. X. Chu is with the School of Electronic and Information Engineering, South China University of Technology, China.

X. X. Yang is with the Shanghai University, China.

TABLE-I
SPECIFICATIONS OF THE DUAL-BAND CP ARRAY ANTENNA

Frequency band	C-band	X-band
Center frequency	5.3 GHz	8.2 GHz
Polarization	right-hand circular polarization (RHCP)	
Impedance bandwidth	800 MHz	
AR bandwidth	500 MHz	
Antenna size	110 mm × 110 mm	
Aperture efficiency	50%	50%
Gain	13 dBic	17 dBic
Cross polarization discrimination (XPD)	20 dB	
Side-lobe level	-12 dB	

aperture is proposed for C/X-band satellite communications. This array uses separate radiation elements and feeding networks for each band. For each element, a novel method of achieving a single-feed broadband CP microsrtip antenna is proposed for the 1st time. This method employs one resonator to excite the two orthogonal modes of the patch via two coupling paths. By using the different orders of the two coupling paths, a coherent 90° phase difference is produced and the CP characteristics are achieved. Compared with the traditional methods, this approach features a compact and simplified feed but delivers the broad impedance and AR bandwidths. All these advantages make it very suitable for the dual-band CP array antenna design with shared aperture. Table I summaries the specifications and design targets of this work. As can be seen, broad impedance and AR bandwidths are simultaneously required at both C- and X-band. In addition, this antenna is required to have a high aperture efficiency, gain, cross polarization discrimination (XPD) and low side-lobe level at both bands. It is noted that right-hand circular polarization (RHCP) at both C- and X-band is required. Other requirements such as low profile, light weight and low cost are also desired.

This paper is organized as follows. Section II describes the configuration and design principles of the proposed dual-band CP array and elements. Section III presents the simulated and measured results, followed by conclusions in Section IV.

II. Configurations and Design Principles

A. Layout of C/X-band shared-aperture CP array

Fig. 1 shows the configuration of the proposed dual-band CP array antenna. The C- and the X-band array are interlaced with each other, sharing the same aperture. The array antenna has a stacked structure, which includes two substrates and a foam spacer between them. The C-band antenna is a 2 × 2 array printed on the top layer of the upper substrate. The X-band antenna is a 4 × 4 array, which is printed on the bottom layer of the upper substrate. It is noted that the circular patches of the C-band are symmetrically etched at the four corners to avoid overlapping with the circular patches of the X-band. This could enhance the isolation between the two bands. The microstrip feed lines with the attached hairpin resonators are

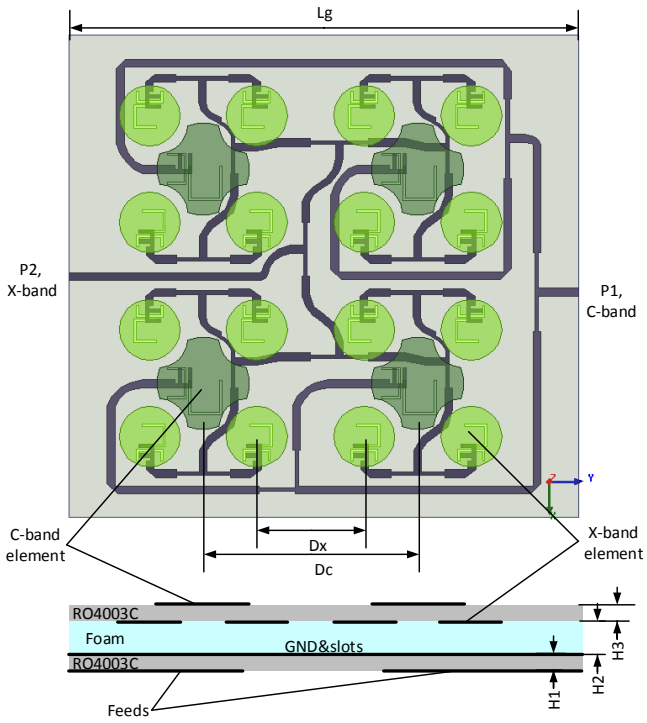

Fig. 1. Configuration of the proposed aperture-shared C/X-band CP microstrip array antenna. *Lg* = 110 mm, *Dx* = 24 mm, *Dc* = 48 mm, *H1* = 0.8 mm, *H2* = 3mm, *H3* = 0.8 mm.

printed on the bottom layer of the lower substrate. The patches and feeding networks share the common ground plane on the top layer of the lower substrate. In the ground, U-shaped slot lines are cut for coupling the electromagnetic energy from the feeds to the radiating patches. There are two U-slots below each patch. The two U-slots are used to produce the CP characteristics, which will be detailed in Section II-B later. It should be noted the feeding networks of the two bands are elaborately designed and constrained in a compact area, which is useful for potential large array antenna designs. RO 4003C substrate with a permittivity of 3.55 and loss tangent of 0.0027 is used in this work. All simulations were performed using the high frequency structural simulator (HFSS 15).

In this work, the distances between the radiation elements of the two arrays were optimized to keep a low grating lobe of -12 dB and a high aperture efficiency of over 50% at both frequency bands. Here, *Dx* = 24 mm (0.65 wavelength at 8.2 GHz) and *Dc* = 48 mm (0.84 wavelength at 5.3 GHz) were chosen.

B. X-band element and generation of CP

Fig. 2 shows the configuration of the broadband X-band CP antenna element. It has a circular patch as the radiation element, which is fed by a single 50 Ω microstrip line via two U-shaped slots (Slot-1 and Slot-2) in the ground. At the end of the microstrip feed, a hairpin resonator is attached and couples with the two U-slots, simultaneously. The two U-slots are oriented perpendicularly to each other so as to stimulate the two orthogonal modes (TM_{11}) of the patch.

It should be noted that the two slots have different

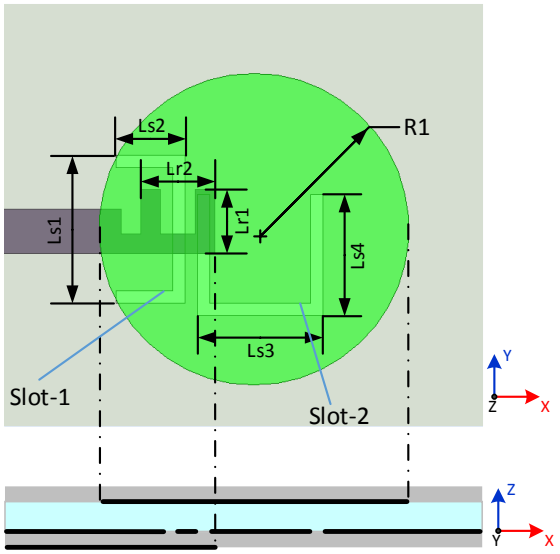

Fig. 2. Configuration of the proposed X-band CP microstrip antenna element. *R1* = 6.8 mm, *Lr1* = 3.4 mm, *Lr2* = 3 mm, *Ls1* = 6 mm, *Ls2* = 3 mm, *Ls3* = 5mm, *Ls4* = 5 mm.

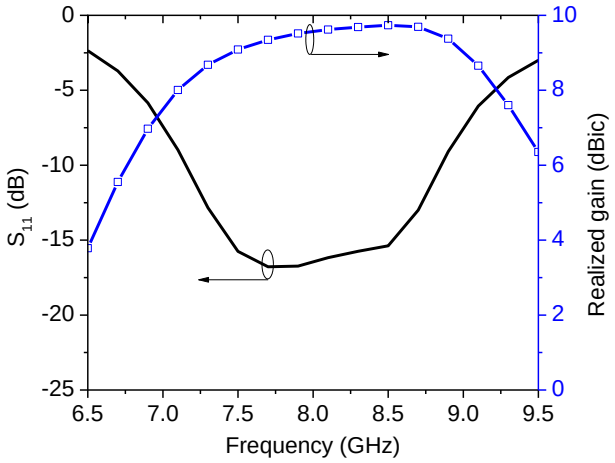

Fig. 3. Simulated S-parameters and antenna gain of the X-band CP antenna element.

dimensions and function differently. Slot-1, which is perpendicular to the hairpin resonator at the center part, is used to couple the electromagnetic energy from the hairpin to the patch and excites the mode in the X-direction. The length of Slot-1 is used to adjust the coupling strength and it does not resonate. The other slot (Slot-2), however, is used to excite the mode in the Y-direction, also works as a resonator. The Slot-2 has the same resonant frequency as the patch. More importantly, this extra resonator provides the 90° phase delay required to generate the circular polarization. Finally, the patch combines the two linearly polarized components with 90° phase difference and produce the CP radiation characteristics. The dimension of Slot-2 can be approximately determined using the following equation,

$$Ls3 + 2 * Ls4 \approx \frac{c}{2 f_0 \sqrt{\varepsilon_{eff}}} \qquad (1)$$

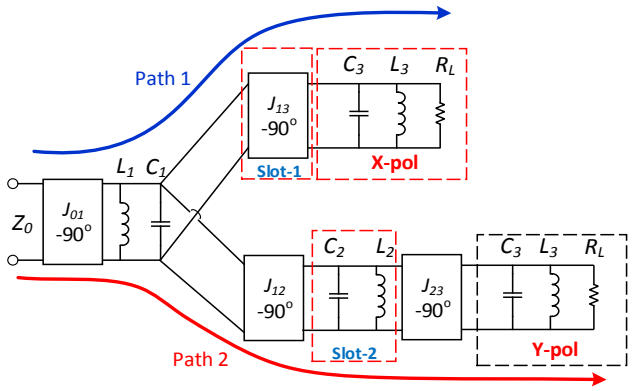

Fig. 4. Equivalent circuit of the proposed CP microstrip antenna element.

where, ε_{eff} is the effective dielectric constants, c is the light speed in free space, f_0 is the resonant frequency of the patch. The optimized parameters are given in the caption of Fig. 2.

Fig. 3 shows the simulated S-parameters and gain of the proposed X-band CP antenna element. A wide impedance bandwidth from 7.2 to 9 GHz (22%) is achieved. This broadband performance is attributed to the integrated resonators and the stacked configuration, which renders a strong coupling between the feed and the patch [21]-[22].

Viewing the gain responses as the function of frequency, we can see that a relatively flat and high gain around 9 dBic is achieved over the broadband. Such a high gain is attributed to the novel single-feed dual coupling-path structure that eliminates the traditional power dividing networks and phase delay lines as well as the associated losses.

C. Equivalent circuit explanation

To illustrate the mechanism of the CP generation, the antenna in Fig. 2 is analyzed using an equivalent circuit, as shown in Fig. 4. The hairpin resonator and the U-slot resonator (Slot-2) are represented by the shunt resonators, L_1C_1 and L_2C_2. Slot-1 does not resonate at the designated frequency and it functions as the admittance inverter J_{13}. The two orthogonal radiating modes of the patch are modeled using a shunt resonator, $R_LL_3C_3$, where R_L is the radiation resistance. The three resonators have the same resonant frequency of f_0. The couplings between them are modeled by the admittance inverters J with a -90° phase delay [23]-[24]. J_{12} represents the coupling between the hairpin and Slot-2; J_{13} represents the coupling between the hairpin and patch via Slot-1; J_{23} represents the coupling between Slot-2 and the patch. The external coupling between the microstrip feed and the hairpin is modeled by J_{01}.

As we can see, there are two coupling paths from the input port to the patch. These two paths individually stimulate the two orthogonal modes of the patch. Path-1 is a 2nd-order resonant circuit, which excites the mode in X-pol. The path-2, however, is a 3rd-order resonant circuit due to the contribution of the resonant Slot-2. The difference in number of resonators (orders) results in the 90° phase difference between the X-pol component and Y-pol component. When the antenna

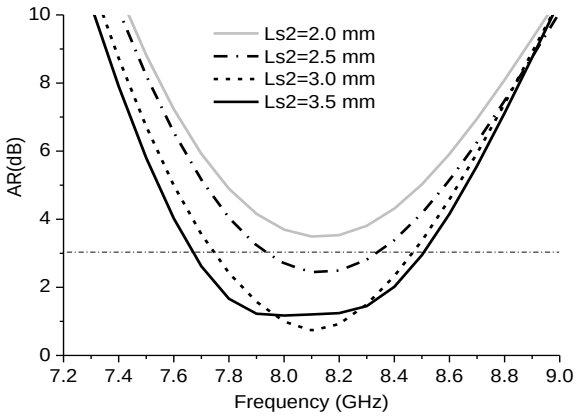

Fig. 5. Simulated AR of the X-band CP antenna element with different lengths of Slot-1, *Ls2*.

combines the two components on the patch, RHCP radiation characteristics can be produced (assuming the antenna radiates in +*Z*-axis direction). To the authors' best knowledge, this is a new technique to achieve the CP characteristics in antennas.

As we know, to generate the CP, the two components in the X-pol and Y-pol must be balanced. This can be adjusted by tuning the coupling strengths of the two coupling paths. Fig. 5 shows the simulated AR of the X-band CP antenna with different lengths of the coupling slot (Slot-1). When *Ls2* is relatively short (less than 2 mm), indicating an inadequate coupling in path-1, the antenna shows a poor CP performance with the AR over 3 dB. As *Ls2* increases, the two components become more balanced, and an improved AR performance can be seen. A 3-dB AR bandwidth of over 900 MHz (11%) is achieved when *Ls2* is 3.5 mm.

D. C/X-band subarray

One of the problems to be overcome in the dual-band array design is how to arrange the radiation elements of the two bands within the same aperture. Fig. 6(a) shows the layout of a C/X-band CP subarray, which is composed of a 2 × 2 X-band array and a C-band element at the center. The C-band element is replotted and shown in Fig. 6(b). The C-band radiation element is a circular patch with four corners, which is used to prevent the overlapping and interference between the two bands. The same single-feed dual-coupling technique is used to generate the circular polarization. The spacing between the C- and X-band element (*R3* - *R1*) is 2.2 mm. It should be noted that even though the shape of the patch is changed, the CP characteristics are still maintained, which provides a flexibility in the dual-band array antenna designs. The other advantage is that the frequency ratio of the high-band to the low-band can be easily adjusted by just changing the *R2*. In this work, a wide range from 1.14 to 1.95 can be achieved. The design parameters are optimized and given in the caption of Fig. 6.

Fig. 7(a) shows the simulated S_{12} of the C/X-band subarray at C-band. At the designated frequency band, $|S_{12}|$ is reduced by more than 6 dB as *R3* increases from 7.5 to 9.5 mm, showing an improved isolation between the two operation bands. However, the cut at the four corners can slightly affect the AR performance of the antenna, as shown in Fig. 7(b). It is

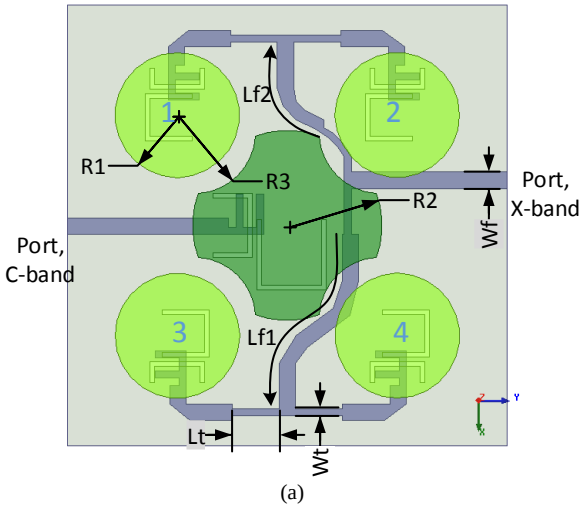

(a)

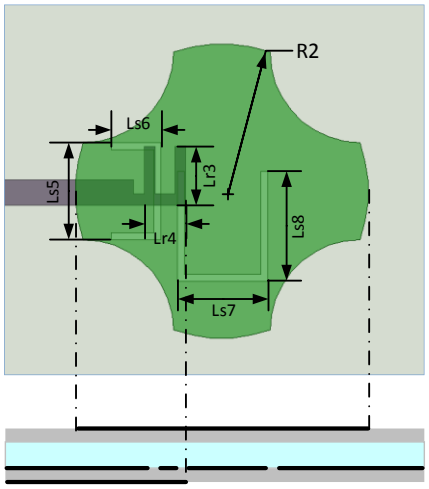

(b)

Fig. 6. (a) Configuration of the C/X-band CP subarray, (b) Configuration of the C-band CP antenna element. *R1* = 6.8 mm, *R2* = 10.3 mm, *R3* = 9 mm, *Lt* = 5.1 mm, *Wt* = 0.8 mm, *Lf1* = 26 mm, *Lf2* = 11.7 mm, *Ls5* = 7 mm, *Ls6* = 4.2 mm, *Ls7* = 7.5 mm, *Ls8* = 7.6 mm, *Lr3* = 4.4 mm, *Lr4* = 3 mm, *Wf* = 1.8 mm.

observed that the simulated AR of the C-band element is deteriorated somewhat when the *R3* increases. As a trade-off between the isolation and AR, *R3* is chosen to be 9 mm in this design.

It is also noted from Fig. 6(a) that the orientations and feed structures of the X-band element-1, 2 are reversed relative to the element-3 and 4. Such an arrangement is to relieve the congestion of the feeding networks on the bottom layer, where the feeds of both arrays are placed. To maintain a consistent phase on each X-band element, an 180^0 phase difference is introduced to the feed lines *Lf1* and *Lf2*. That is,

$$Lf1 - Lf2 \approx \frac{\lambda_g}{2} \tag{2}$$

where λ_g is the guide wavelength at 8.2 GHz.

Fig. 8 shows the simulated current distribution on the patches of the subarray at the two operation frequencies. As can be observed, the antenna exhibits the CP current distribution characteristics at both operations. At 5.3 GHz (C-

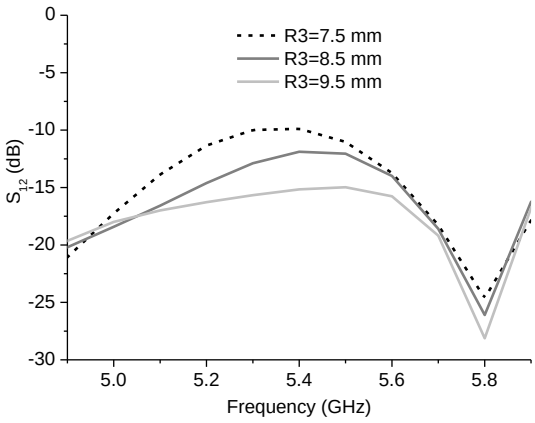

(a)

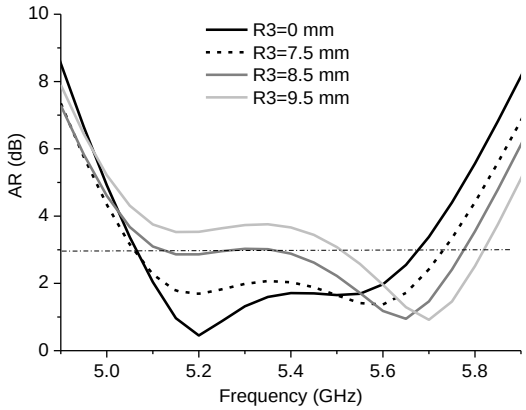

(b)

Fig. 7. (a) Simulated S_{12} of the subarray with different *R3*, (b) simulated AR of the C-band element with different *R3*.

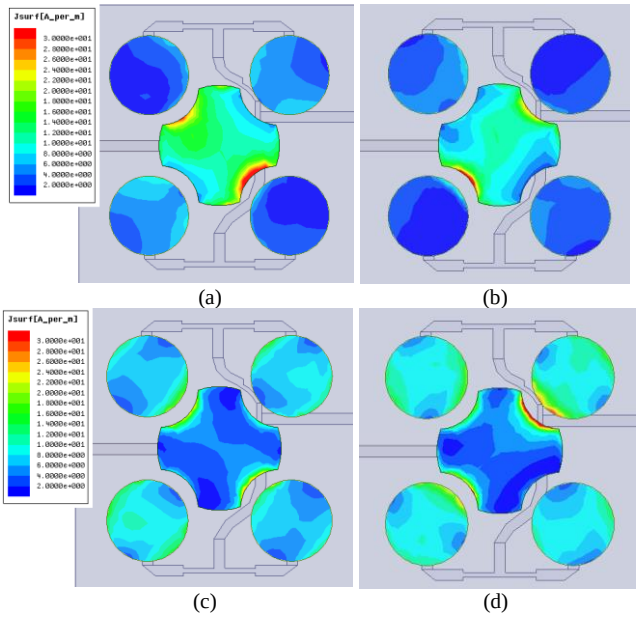

(a) (b)

(c) (d)

Fig. 8. Current distribution of the dual-band CP subarray at: (a) 5.3 GHz, t = 0, (b) 5.3 GHz, t = T/4, (c) 8.2 GHz, t = 0, (d) 8.2 GHz, t = T/4.

band), the current is mainly distributed on the central patch and the current on the surrounding four patches are very weak. When the X-band array is excited at 8.2 GHz, however, the current is mainly distributed on the four smaller patches.

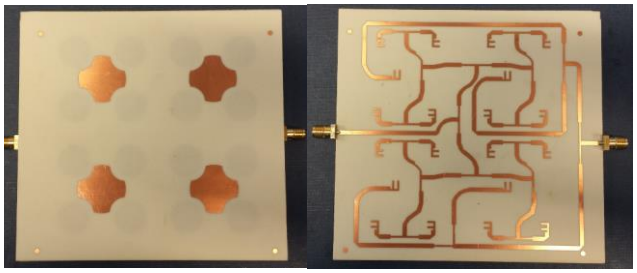

(a) (b)

Fig. 9. Prototype of the C/X-band CP array antenna: (a) front view, (b) back view.

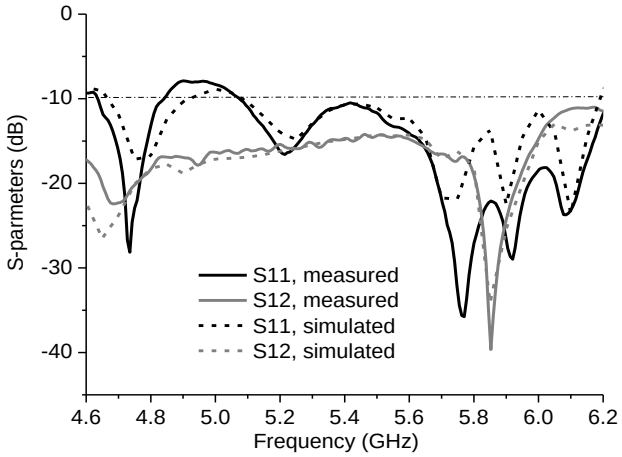

Fig. 10. Simulated and measured S-parameters of the dual-band CP array antenna at C-band.

III. Results and Discussion

The C/X-band CP array antenna was prototyped and tested to verify the design concept. Fig. 9 presents the front view and back view of the prototype. The simulated and measured S-parameters of the array antenna at C-band are shown in Fig. 10. As can be observed, a very good agreement between the measurements and simulations is achieved, showing a broad -10 dB impedance bandwidth from 5.0 to 6.2 GHz (FBW = 21%). The measured isolation around 5.3 GHz is higher than 15 dB. The minor discrepancy is mainly caused by the fabrication tolerance.

Fig. 11 shows the simulated and measured S-parameters of the array antenna at X-band. The measured result agrees very well with the simulation, showing an impedance bandwidth from 7.2 to 8.9 GHz (FBW = 21.2%). The measured bandwidth is slightly wider than the simulated one. At the designated operation band between 7.9 and 8.4 GHz, the reflection coefficient is below -20 dB. The simulated and measured isolation around the X-band is over 20 dB.

Fig. 12 shows the measured and simulated AR of the proposed C/X-band CP microstrip array antenna in the boresight direction. The AR was measured by rotating the antenna a circle and calculating the difference between the maximum and minimum received power. When P1 is excited, the antenna exhibits a 3-dB AR bandwidth from 4.95 to 5.65 GHz (FBW = 13.2%) for C-band operation. The measured

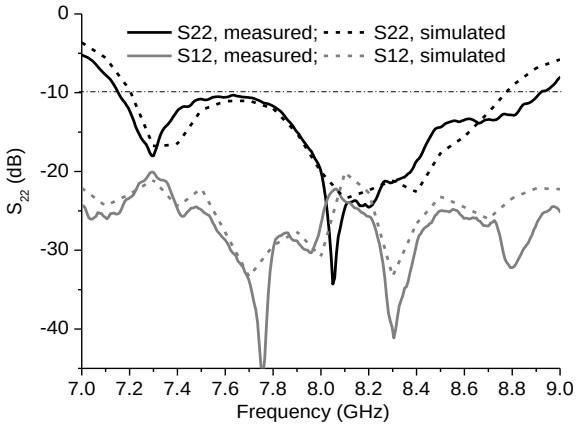

Fig. 11. Simulated and measured S-parameters of the dual-band CP array antenna at X-band.

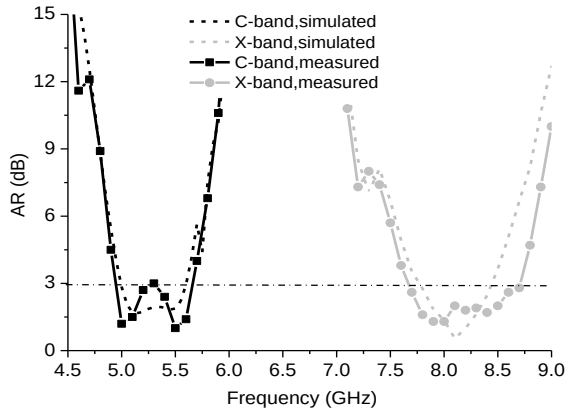

Fig. 12. Simulated and measured AR of the proposed C/X-band CP array antenna.

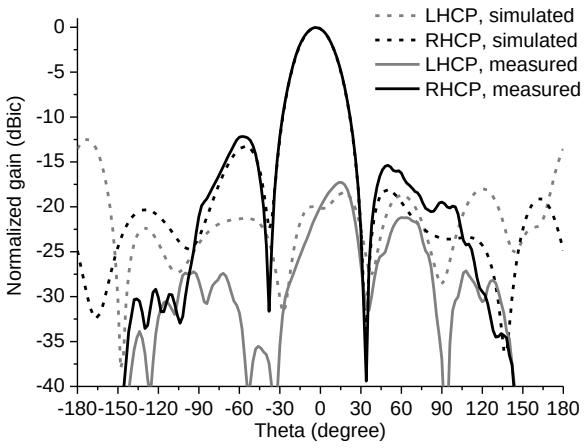

(a)

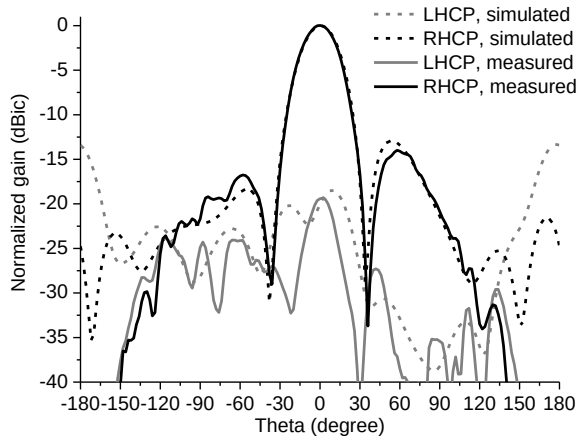

(b)

Fig. 13. Measured and simulated normalized radiation patterns of the C/X-band CP array antenna at 5.3 GHz: (a) φ = 0°, (b) φ = 90°.

bandwidth is slightly wider than the simulated one, which may be attributed to the fabrication and measurement tolerances. When P2 is excited (X-band array), the antenna has a 3-dB AR bandwidth from 7.65 to 8.7 GHz (FBW = 12.8%). Similarly, the measured bandwidth is slightly wider than the simulation. It is noted that the 3-dB AR bandwidths are entirely situated within the corresponding impedance bandwidths of the two bands.

Fig. 13 shows the simulated and measured normalized radiation patterns of the proposed C/X-band CP array antenna at 5.3 GHz when P1 is excited and P2 is terminated with a 50 Ω load. The measured results agree very well with the simulations with the main beam in the broadside direction, showing the RHCP radiation characteristics. In φ = 0° plane, the measured XPD in broadside direction is higher than 19 dB, and the measured sidelobe is below -12.5 dB. In φ = 90° plane, as shown in Fig. 13(b), the measured XPD is over 20 dB and the sidelobe is lower than -14 dB. The minor discrepancy between the measured and simulated results is attributed to the measurement tolerances.

Fig. 14 shows simulated and measured normalized radiation patterns at 8.2 GHz when the X-band array is excited. As can be seen, very good RHCP radiation characteristics are achieved. In both planes, the measured XPD is over 20 dB in the broadside direction. The measured sidelobes are lower than -15 dB. Compared with the patterns of C-band array, the X-band array shows a lower sidelobe, which is attributed to the relatively short distance between the X-band elements.

Fig. 15 shows the simulated and measured realized gain of the proposed shared-aperture C/X-band CP array antenna in the broadside direction. When the C-band array is excited, the antenna exhibits a high gain of over 13 dBic over a broadband from 5 to 5.6 GHz. At the designated frequency of 5.3 GHz, the measured gain is 14.5 dBic. When the X-band array is excited, the antenna has a gain of 17.5 dBic from 7.5 to 8.7 GHz. The measured gain at 8.2 GHz is 18 dBic. The aperture efficiency of the antenna at the two operation bands can be calculated using the formula,

$$e = \frac{G\lambda^2}{4\pi \cdot A_{phys}} \qquad (3)$$

where e is the aperture efficiency, G is the gain of the antenna, A_{phys} is the physical area of the antenna aperture. Using the measured results, the aperture efficiency at C- and X-band can be calculated to be 59.4% and 55.6%, respectively.

Table II compares the proposed shared-aperture dual-band CP microstrip antenna with the other four reported dual-band CP array antennas in [15]-[18]. The comparison focuses on the

TABLE II
COMPARISON WITH OTHER DUAL-BAND CP ARRAYS

Antennas	Operation bands (GHz)	Impedance bandwidth	3-dB AR bandwidth	Gain (dBic)	Aperture efficiency	XPD (dB)	Side-lobe level (dB)
[15]	2.5; 2.65	2%; 1.9%	1.0%; 0.7%	7.0; 7.0	28.6%; 27.2%	-	-
[16]	4.0; 6.0	25%; 13.8%	-	11.0; 12.0	25%; 14%	24.0; 25.0	-12.0; -8.0
[17]	12.2; 17.5	8.3%; 18.9%	14.2%; 14.9%	17.0; 18.0	53.1%; 32.4%	15.0; 16.0	-9.0; -10.0
[18]	2.53; 3.6	3.6%; 3.3%	0.67%; 0.6%	10.8; 12.5	65%; 46%	18.0; 17.0	-20.0; -11.0
This work	5.3; 8.2	21%; 21.2%	13.2%; 12.8%	14.5; 17.5	59.4%; 55.6%	19.0; 20.0	-12.5; -15.0

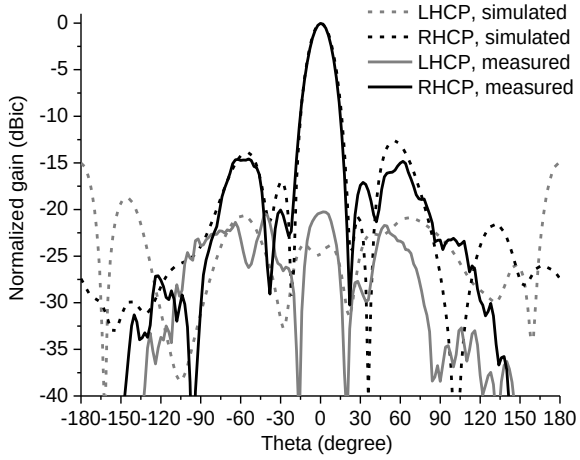

(a)

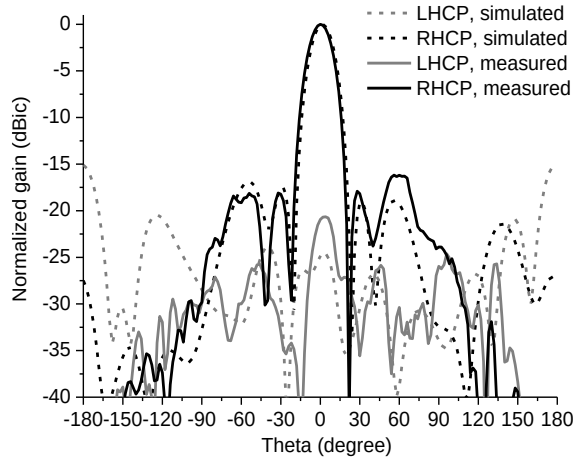

(b)

Fig. 14. Measured and simulated normalized radiation patterns of the C/X-band array antenna at 8.2 GHz: (a) φ = 0°, (b) φ = 90°.

impedance bandwidth, 3-dB AR bandwidth, antenna gain, aperture efficiency, XPD and the side-lobe level. This comparison demonstrates that the proposed antenna has the wider impedance and AR bandwidths than the antennas in [15], [16] and [18]. The antenna in [17] shows the broad AR bandwidths at the two bands, but the aperture efficiency at the high-band operation is relatively low (32.4%). This is resulted from the identical radiation elements at both bands. This also leads to a deteriorated pattern with a higher side-lobe at the high band. For the array antenna in this work, the aperture efficiency at both band are over 55%, and the side-lobes are lower than -12.5 dB. The comparisons demonstrates that the proposed dual-band CP array has achieved improved performance compared to other reported works.

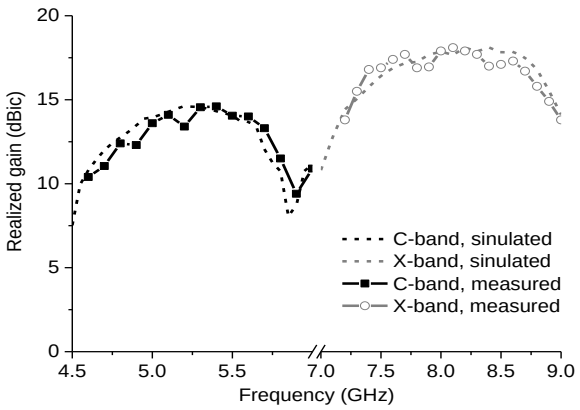

Fig. 15. Simulated and measured realized gain of the shared-aperture C/X-band CP array antenna.

IV. CONCLUSION

In this paper, a compact dual-band CP microstrip array antenna with the shared-aperture was proposed for C/X-band satellite communications. This antenna was implemented based on a novel technique of achieving CP using a single-feed dual-coupling structure. To the author's best knowledge, this technique is reported for the 1st time. The array antenna has a compact size but exhibits good performance in terms of impedance bandwidths, 3-dB AR bandwidths, aperture efficiencies, antenna gains, XPD, and the side-lobe levels at both bands. The design method and its equivalent circuit were analyzed and discussed. In addition, the configuration of the C-band element and the layout of the C/X-band subarray were investigated with the consideration of channel isolation and AR performance. The prototype was developed and the measured results agree with the simulations with all the desired specifications fulfilled.

REFERENCES

[1] W. A. Imbriale, S. Gao, and L. Boccia (eds), Space Antenna Handbook, Wiley, 2012.

[2] S. Gao, Q. Luo and F. Zhu, Circularly Polarized Antennas, IEEE Press & Wiley, 2014

[3] L. Shafai, W. Chamma, M. Barakat, P. Strickland and G. Seguin, "Dual-band dual-polarized perforated microstrip antennas for SAR application," *IEEE Trans. Antennas and Propag*., vol. 48, no. 1, pp. 58-66, Jan. 2000.

[4] D. M. Pozar, S. D. Targonski, "A shared-aperture dual-band dual polarized microstrip array," *IEEE Trans. Antennas and Propag*., vol. 49, no. 2, pp. 150-157, Feb. 2001.

[5] C. H. Chen and E. K. N. Yung, "Dual-band circularly-polarized CPW-fed slot antenna with a small frequency ratio and wide bandwidths," *IEEE Trans. Antennas Propag*., vol. 59, no. 4, pp. 1379–1384, Apr. 2011.

[6] X. Bao, M. Ammann, "Dual-frequency dual-sense circularly-polarized slot antenna fed by microstrip Line," *IEEE Trans. Antennas Propag*., vol. 56, no. 3, pp. 645–649, Mar. 2008.

[7] Y. Shao, Z. Chen, "A design of dual-frequency dual-sense circularly-polarized slot antenna," *IEEE Trans. Antennas Propag*., vol. 60, no. 11, pp. 4992–4997, Nov. 2012.

[8] Nasimuddin, Z. N. Chen, and X. Qing, "Dual-band circularly polarized S-shaped slotted patch antenna with a small frequency-ratio," *IEEE Trans. Antennas Propag*., vol. 58, no. 6, pp. 2112–2115, Jun. 2010.

[9] F. Ferrero, C. Luxey, G. Jacquemod and R. Staraj, "Dual-band circularly polarized microstrip antenna for satellite applications," *IEEE Antennas Wireless Propag. Lett*., vol. 4, pp. 13-15, 2005.

[10] D. Sanchez and I. Robertson, "Analysis and design of a dual-band circularly polarized microstrip antenna," *IEEE Trans. Antennas Propag*., vol. 43, no. 2, pp. 201–205, Feb. 1995.

[11] D. Pozar, S. Muffy, "A dual-band circularly polarized aperture-coupled stacked microstrip antenna for global positioning satellite," *IEEE Trans. Antennas Propag*., vol. 45, no. 11, pp. 1618–1625, Nov. 1997.

[12] T. N. Chang and J. M. Lin, "Serial aperture-coupled dual band circularly polarized antenna," *IEEE Trans. Antennas Propag*., vol. 59, no. 6, pp. 2419–2423, Jun. 2011.

[13] K. P. Yang, K. L. Wong, "Dual-band circularly-polarized square microstrip antenna," *IEEE Trans. Antennas Propag*., vol. 49, no. 3, pp. 377–382, Mar. 2001.

[14] R. Caso, A. Michel, M. Rodriguez and P. Nepa, "Dual-band UHF-RFID WLAN circularly polarized antenna for portable RFID readers," *IEEE Trans. Antennas Propag*., vol. 62, no. 5, pp. 2822–2826, May 2014.

[15] J. T. S. Sumantyo, K. Ito, and M. Takahashi, "Dual-band circularly polarized equilateral triangular-patch array antenna for mobile satellite communications," *IEEE Trans. Antennas Propag*., vol. 53, no. 11, pp. 3477–3485, Nov. 2005.

[16] A. B. Smolders, R. M. C. Mestrom, A. C. F. Reniers, and M. Geurts, "A Shared aperture dual-frequency circularly polarized microstrip array antenna," *IEEE Antennas Wireless Propag. Lett*., vol. 12, pp. 120-123, 2013.

[17] J. D. Zhang, W. Wen, and D. G. Fang, "Dual-band and dual-circularly polarized shared-aperture array antennas with single-layer substrate," *IEEE Trans. Antennas Propag*., vol. 64, no. 1, pp. 109–116, Jan. 2016.

[18] J. D. Zhang, L. Zhu, N. W. Liu and W. Wen, "Dual-band and dual-circularly polarized single-layer microstrip array based on multiresonant modes," *IEEE Trans. Antennas Propag*., vol. 65, no. 3, pp. 1428–1433, Mar. 2017.

[19] C. X. Mao, S. Gao, Y. Wang, Q. Luo, Q. X. Chu, "A shared-aperture dual-band dual-polarized filtering-antenna-array with improved frequency response," *IEEE Trans. Antennas and Propag.*, vol. 65, no. 4, pp. 1836-1844, Apr. 2017.

[20] C. X. Mao, S. Gao, Q. Luo, T. Rommel, Q. X. Chu, "Low-cost X/Ku/Ka-band dual-polarized array with shared-aperture," *IEEE Trans. Antennas and Propag.*, vol. 65, no. 4, pp. 1836-1844, Apr. 2017.

[21] C. X. Mao, S. Gao, Y. Wang, F. Qin, Q. X. Chu, "Multimode resonator-fed dual-polarized antenna array with enhanced bandwidth and selectivity," *IEEE Trans. Antennas and Propag.*, vol. 63, no. 12, pp. 5493-5499, Dec. 2015.

[22] C. X. Mao, S. Gao, Y. Wang, Z. Wang, F. Qin, B. Sanz, Q. X. Chu, "A integrated filtering antenna array with high selectivity and harmonics suppression," *IEEE Trans. Microw. Theory and Techn..*, vol. 65, no. 4, pp. 1836-1844, Apr. 2017.

[23] J. S. Hong and M. J. Lancaster, *Microwave Filter for RF/Microwave Application*. New York: Wiley, 2001.

[24] C. K. Lin and S. J. Chung, "A Filtering Microstrip Antenna Array," *IEEE Trans. Microw. Theory Techn., vol.* 59, no. 11, pp. 2856-2863, Mar. 2011.

Chun-Xu Mao was born in Hezhou, Guangxi, China. He received the M.S. degree in RF and microwave engineering from South China University of Technology in 2013. He is currently working toward the Ph.D. degree at University of Kent, U.K. His research interests include UWB antenna, filtering antenna, circularly-polarized antenna, integration of passive devices, antenna array for satellite communication and space-borne synthetic aperture radar.

Steven (Shichang) Gao (M'01–SM'16) is a Professor and Chair of RF and Microwave Engineering at University of Kent, UK. His research covers smart antennas, phased arrays, MIMO, satellite antennas, RF/microwave/mm-wave circuits, satellite communications, UWB radars, synthetic-aperture radars and mobile communications. He has two books including <<Space Antenna Handbook>> (Wiley, 2012) and <<Circularly Polarized Antennas>> (IEEE-Wiley, 2014), over 200 papers and several patents. He is an IEEE AP-S Distinguished Lecturer, an Associate Editor of *IEEE Transactions on Antennas and Propagation*, an Associate Editor of *Radio Science* and the Editor-in-Chief for Wiley Book Series on "Microwave and Wireless Technologies". He was General Chair of LAPC 2013, and a Keynote Speaker or Invited Speaker at some international conferences such as AES'2014 (China), IWAT'2014 (Sydney), SOMIRES'2013 (Japan), APCAP'2014 (China), etc.

Yi Wang (M'09–SM'12) received the B.Sc. degree in Physics and M.Sc. degree in Condensed Matter Physics from the University of Science and Technology, Beijing, China, in 1998 and 2001, respectively, and the Ph.D. degree in Electronic and Electrical Engineering from The University of Birmingham, in 2005. In 2011, he became a Senior Lecturer at the University of Greenwich in the UK. His present research interests include millimeter-wave/terahertz devices for metrology, communications and sensors, microwave circuits based on multi-port filtering networks, and antennas.

Qing-Xin Chu (M'99–SM'11) received the B.S, M.E., and Ph.D. degrees in electronic engineering from Xidian University, China, in 1982, 1987, and 1994, respectively. He is currently a Full Professor with the School of Electronic and Information Engineering, South China University of Technology, Guangzhou, Guangdong, China. He is also the Director of the Research Institute of Antennas and RF Techniques, South China University of Technology. Prof. Chu is a fellow of the China Electronic Institute (CEI). He was the recipient of the Tan Chin Tuan Exchange Fellowship Award, a Japan Society for Promotion of Science (JSPS) Fellowship, the 2002 and 2008 Top-Class Science Award of the Education Ministry of China, and the 2003 First-Class Educational Award of Shaanxi Province. His current research interests include antennas in wireless communication, microwave filters, spatial power combining array, and numerical techniques in electromagnetics.

Xue-Xia Yang is a Professor at School of Communication and Information Engineering, Shanghai University, China.